Journal of Non-Crystalline Solids 358 (2012) 2520–2524

Contents lists available at SciVerse ScienceDirect

Journal of Non-Crystalline Solids

journal homepage: www.elsevier.com/ locate/ jnoncrysol

Real-time ellipsometric characterization of the initial growth stage of poly(3,4-ethylenedioxythiophene):poly(styrene sulfonate) films by electrospray deposition using *N*,*N*-dimethylformamide solvent solution

Tomohisa Ino, Taiga Hiate, Takeshi Fukuda, Keiji Ueno, Hajime Shirai *

Graduate School of Science and Engineering, Saitama University, 255 Shimo-Okubo, Sakura-ku, Saitama 338–8570, Japan

ARTICLE INFO

Article history:
Received 14 July 2011
Received in revised form 25 January 2012
Available online 12 March 2012

Keywords:
PEDOT:PSS;
DMF;
Spectroscopic ellipsometry;
Real-time monitoring;
Electrospray deposition

ABSTRACT

The initial growth stage of poly(3,4-ethylenedioxythiophene):poly(styrene sulfonate) (PEDOT:PSS) films by the electrospray deposition (ESD) method was investigated using 70% *N*,*N*-dimethylformamide (DMF) as a solvent solution through the real-time spectroscopic ellipsometric (SE) characterization. The uniaxial anisotropic optical property was prominent for the film growth on c-Si wafer, whereas the homogeneous growth occurred with random molecular orientation on indium-tin-oxide (ITO) coated glass. These findings probably originate from a preferential orientation of the polymer chains as obtained in the preparation process, sort of substrate, its morphology, and film thickness.

1. Introduction

Poly(3,4-ethylenedioxythiophene)-poly(styrene sulfonate) (PEDOT:PSS) is among the most successful conjugated polymers to be used commercially in organic electroluminescence (EL) materials and organic thin-film solar cell (OSC) devices as a hole transport layer [1]. That is also one of most promising organic-based electrode materials by mixing polar solvent such as *N*,*N*-dimethylformamide (DMF), dimethyl sulfoxide (DMSO), and graphene oxide (GO) owing to its inherent advantages over other conducting polymers such as high stability in the p-doped form, high conductivity, good film-forming properties, and/or excellent transparency in the visible range, long-term stability, and solution processability [2–7]. In particular, PEDOT:PSS dispersed in water can easily be spin-coated to produce transparent films with a high electrical conductivity (typically 0.05–10 S/cm) and a low sheet resistance. In the PEDOT:PSS dispersion the polymer chains are likely to adopt a random coil conformation. When such a dispersion is coated onto substrate, a thin polymer film is formed, with grains consisting of doped conjugated polymer coil. Since PSS chains typically consist of a few hundred monomer units, the polymer grains possibly consists of neutral species, i.e., excess PSS. Thus, the depth profile of the film morphology is an interesting feature, i.e., uniaxial anisotropic optical property and electrical conductivity to analyze, especially given the major role played by granularity and disorder in the conduction of conjugated polymers. To date, most of studies on the film synthesis and optical anisotropic property of PEDOT:PSS films have been performed using the spin-coating method [7–9]. In comparison, the influence of film thickness and sort of substrate on optical anisotropic property is still controversial for the PEDOT:PSS films fabricated by the dry-processing such as spray coating and ink jet printing [10].

In this paper, we demonstrate the real-time monitoring of optical anisotropy in PEDOT:PSS films on c-Si and indium-tin-oxide (ITO) coated glass substrates using DMF as a solvent solution by the ESD method monitored by UV-visible SE.

2. Experimental details

A schematic of the experimental setup for the ESD is shown in Fig. 1. Inset shows the molecular structure of PEDOT:PSS and the Mie scattering image of ESD jet of PEDOT:PSS diluted in DMF solvent. The DMF solvent added to an aqueous solution of PEDOT:PSS was used as a precursor and its was contained in a glass capillary of 80 μm diameter and 3 cm length. A positive dc bias of 12 kV was supplied to the aqueous solution of PEDOT:PSS directly through a tungsten wire. The capillary-substrate distance, *D*, was 20 mm. The film deposition was performed on a 2.1-nm-thick native oxide-coated c-Si wafer and ITO coated glass substrates.

Real-time measurements of the ellipsometric angles, Ψ and Δ, defined as complex reflection ratio, $\rho = R_p/R_s = \tan\psi \cdot \exp(i\Delta)$, were made for 32 different photon energies between 1.0 and 5.0 eV after interval of 1 s and an integration time of 200 ms during a film deposition period of 40 s. Where R_p and R_s are reflection

* Corresponding author. Tel./fax: +81 48 858 3676.
E-mail address: shirai@fms.saitama-u.ac.jp (H. Shirai).

0022-3093/$ – see front matter © 2012 Elsevier B.V. All rights reserved.
doi:10.1016/j.jnoncrysol.2012.01.055

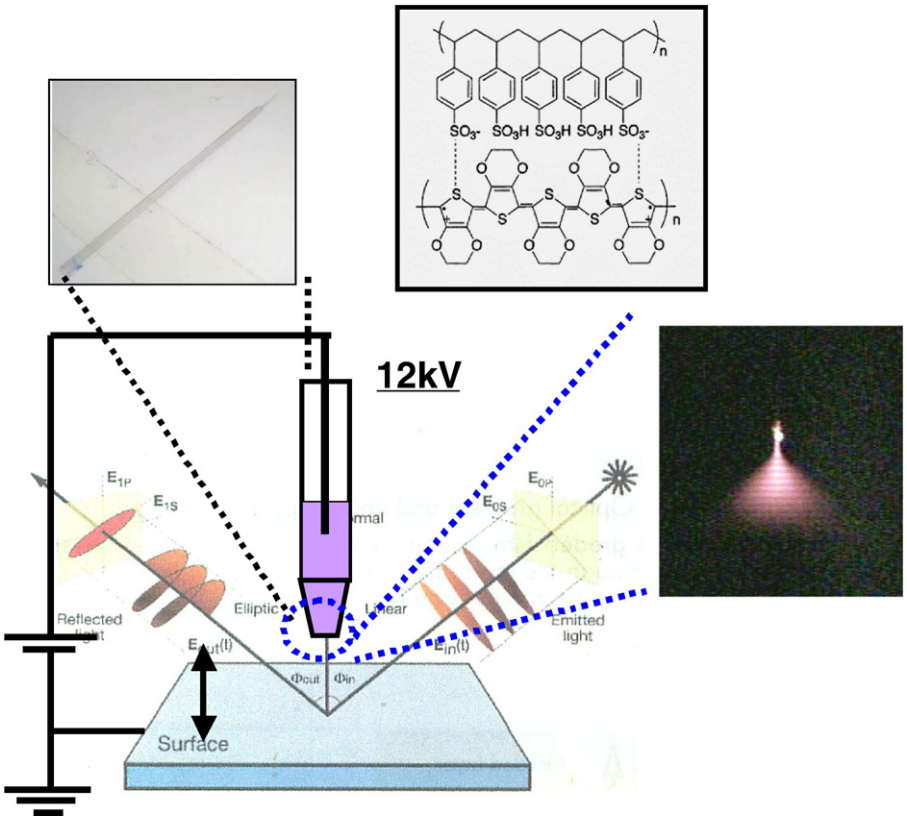

Fig. 1. Schematic of the apparatus used for the ESD. Inset shows the molecular structure of PEDOT:PSS and the Mie scattering image of ESD jet of PEDOT:PSS diluted in DMF solvent at the tip of the capillary tube.

coefficients for a linearly polarized light, parallel and perpendicular to the plane of incidence. The angle of incidence of probe light θ_i was 70°. The variable angle SE was also used for the ex situ measurement at θ_is of 55–75°. These spectra were analyzed using a linear combination of a Tauc–Lorentz (TL) oscillator and effective medium approximation (EMA) as follows [11,12]:

$$\varepsilon(E) = \varepsilon_1 + i\varepsilon_2 = \varepsilon_{1\infty} + \begin{cases} \frac{1}{E}\frac{AE_0C\left(E-E_g\right)^2}{\left(E^2-E_0^2\right)^2+C^2E^2} & \text{for } E > E_g \\ 0 & \text{for } E \le E_g \end{cases}, \qquad (1)$$

where $\varepsilon_{1\infty}$ is the background high-frequency dielectric constant and ε_1 and ε_2 are the real and imaginary parts of the complex dielectric function, respectively. Optical model used for the spectra analysis was a single-layer model with ordinary and extraordinary index of reflection (n_o and n_e), and of extinction coefficient (k_o and k_e) parameter set ($\varepsilon_{1\infty}$, A, C, E_0, E_g) for PEDOT:PSS components, the volume fractions of PEDOT:PSS and void, $f_{PEDOT:PSS}$, f_{void} for ordinary and extraordinary component, and the total film thickness d as free parameters (Fig. 2). The numerical calculation was performed by minimizing the measurement and calculated values, χ^2 using a least square method [13,14].

3. Results

Fig. 3a shows the measured $<n>$ and $<k>$ spectra of a 30-nm-thick ESD-deposited PEDOT:PSS film from the 70% DMF solvent solution on c-Si wafer at different θ_is. The best-fitted n_o, n_e, k_o, and k_e spectra obtained from the spectra fitting procedure measured at $\theta_i = 70°$ are shown in Fig. 3b. The n_o showed metallic behavior, which could be interpreted to correspond to a high conductivity for the material. In comparison, the n_e showed features more characteristic of a dielectric material as was similar to those of spin-coated PEDOT:PSS film[7]. They also included f^o_{void} and f^e_{void} of 55 and 38%, respectively. These large volume fractions of void originate from the deposition kinetics and/or change of microstructure due to residual solvent material DMF by the ESD method.

The real-time SE data collected during the preparation of a PEDOT:PSS films fabricated with a 70% concentrated DMF solvent on a native oxide-covered crystalline Si (c-Si) wafer and ITO coated glass during the initial 40 s growth are shown in Fig. 4. Here, 60 pairs of $<n>$ and $<k>$ are an alternative way of expressing the ellipsometric data and is deduced directly from $\rho = R_p/R_s = \tan\psi \cdot \exp(i\Delta)$. The $<n>$ and $<k>$ spectra at $t = 0$, corresponding to those of c-Si showed fine structures at 3.3 and 4.2 eV attributing to E_1 and E_2 optical interband transitions, respectively, and their structures became obscure with deposition time due to the PEDOT:PSS film deposition. The magnitude of $<n>$ and $<k>$ at the UV energy regions decreased with deposition period more rapidly, because they were sensitive to the film surface roughness rather than to the bulk. Thus, these $<n>$ and $<k>$ spectra, in general, in-

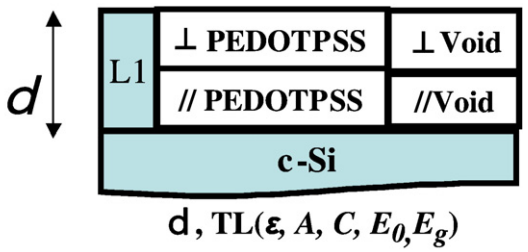

Fig. 2. Optical model used for the spectra analysis.

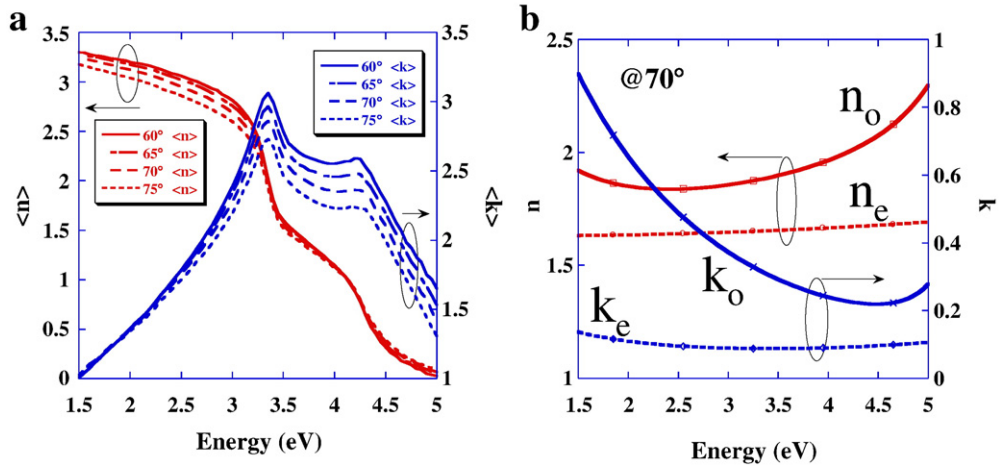

Fig. 3. (a) Spectroscopic $<n>$ and $<k>$ spectra of an 30-nm-thick ESD-deposited PEDOT:PSS films from the 70% DMF solvent solution on a native oxide covered c-Si as open circles. (b) The best-fitted result calculated using a TL oscillator and a Drude oscillator is shown as a solid line.

clude the information of optical constant of bulk and substrate including the homogeneity and surface roughness.

Fig. 5a and b shows the time evolutions of $n_{o(e)}$ and $k_{o(e)}$ spectra of bulk PEDOT:PSS component on c-Si and changes of d, $f_{void}^{o(e)}$, and χ^2 determined by the spectra fitting procedure during the first 40 s on c-Si wafer and ITO coated glass. Both isotropic and anisotropic single-layer model was used for the spectra analysis and the χ^2 value was lower for the use of anisotropic optical model in both c-Si and ITO substrates. The d increased linearly from the first stage with a 1 nm/s on c-Si wafer and a 0.8 nm/s on ITO coated glass. The $n_{o(e)}$ and $k_{o(e)}$ increased up to ~25 nm thickness, and subsequently, they tend to saturate with prominent feature of optical anisotropy on c-Si. Once both f_{void}^{o} and f_{void}^{e} increased up to 90–95% and they decreased gradually to 50(ordinary) and

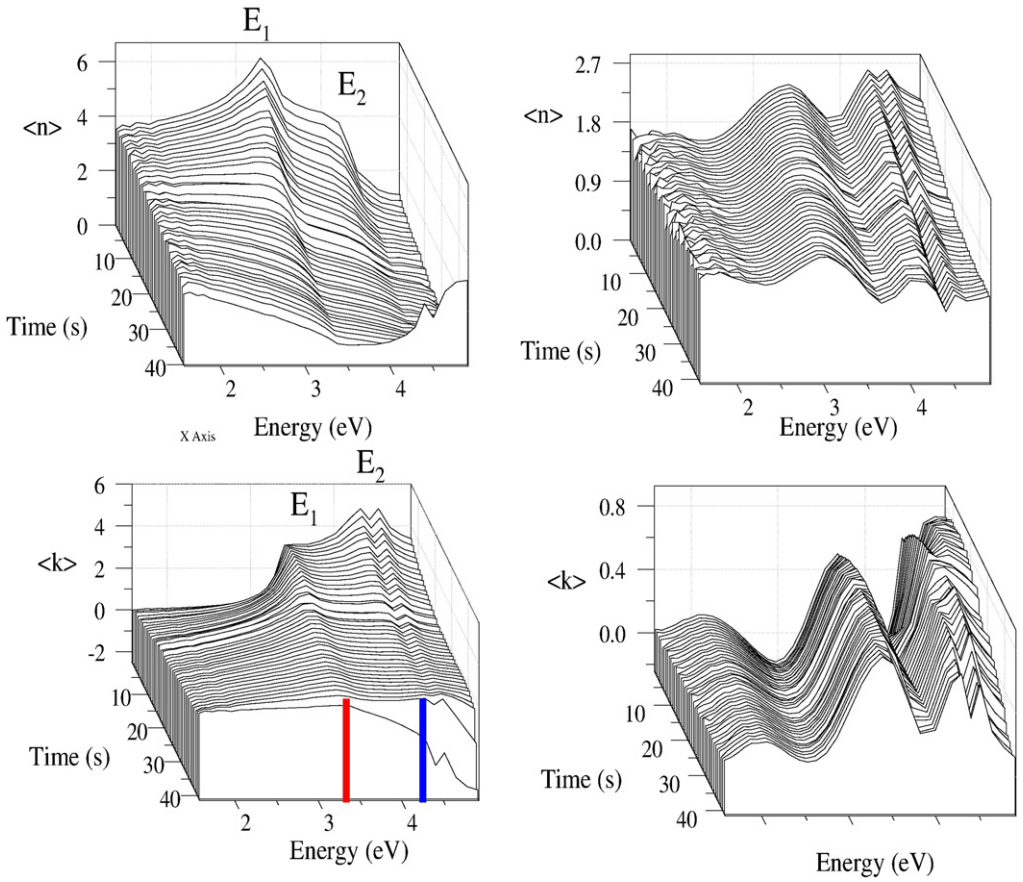

Fig. 4. Time evolution of $<n>$ and $<k>$ spectra during the initial growth stage of PEDOT:PSS films on c-Si wafer and ITO coated glass using a 70% DMF diluted solution by the ESD method.

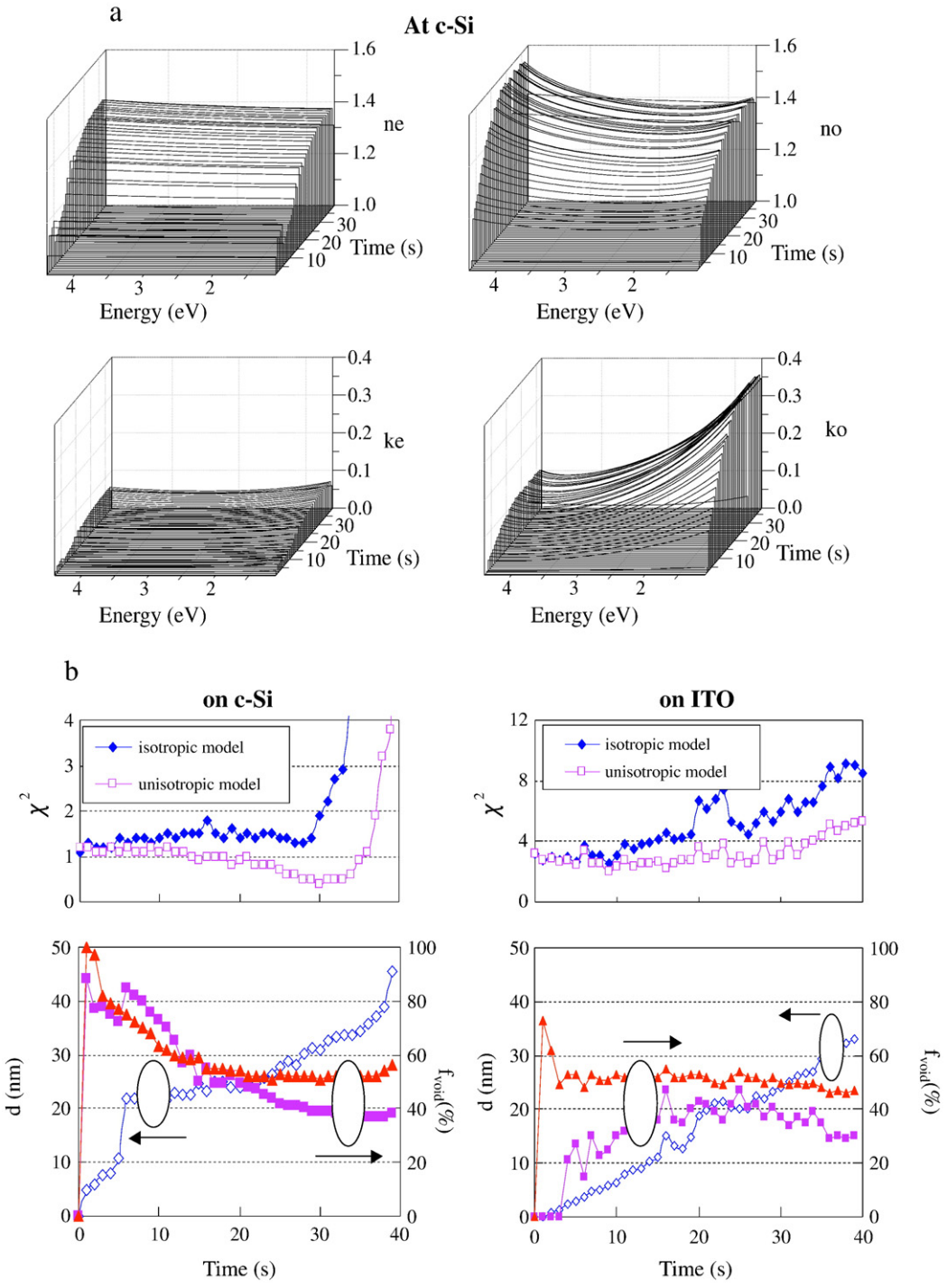

Fig. 5. (a) Time evolutions of n_o, n_e, k_o, and k_e spectra during the initial 40-s film deposition on c-Si and ITO coated glass. (b) Changes of total film thickness d, f^o_{void}, f^e_{void}, and χ^2 with deposition period for the films on c-Si and ITO coated glass.

38% (extraordinary) with film thickness, indicating a promoting the cross-linking reaction of conjugated polymer chain. Subsequently, bothf^o_{void} and f^e_{void}were almost independent of film thickness up to 30–40 nm. Whereas, the degree of the optical anisotropy was lower on ITO coated glass, which was almost independent of deposition period. Thus, homogeneous growth occurred from the first stage. The χ^2 values of 1.1–1.2 were also almost independent of film thickness up to a ~30 nm on c-Si wafer and of 2–3 on ITO coated glass. Thus, the uniaxial anisotropic optical property depends on a sort of substrate as well as film thickness.

Fig. 6 shows the grazing incidence X-ray diffraction (GI-XRD) pattern of the ESD PEDOT:PSS films with different film thicknesses on c-Si wafer and ITO coated glass substrates. The first-order Bragg diffraction peak corresponding to $2l\sin\theta = n\lambda$ (l. lattice constant, $n = 1$) appeared on c-Si as a broad band peak corresponding l of 3.2 nm in the films. On the contrary, n_o significant specific features were observed in the films deposited on ITO. These features are qualitatively consistent with the result of Fig. 5. These findings suggest that the uniaxial anisotropic optical property is determined by the preferential molecular orientation on c-Si wafer, whereas the growth of polymer chain proceeds randomly on ITO coated glass.

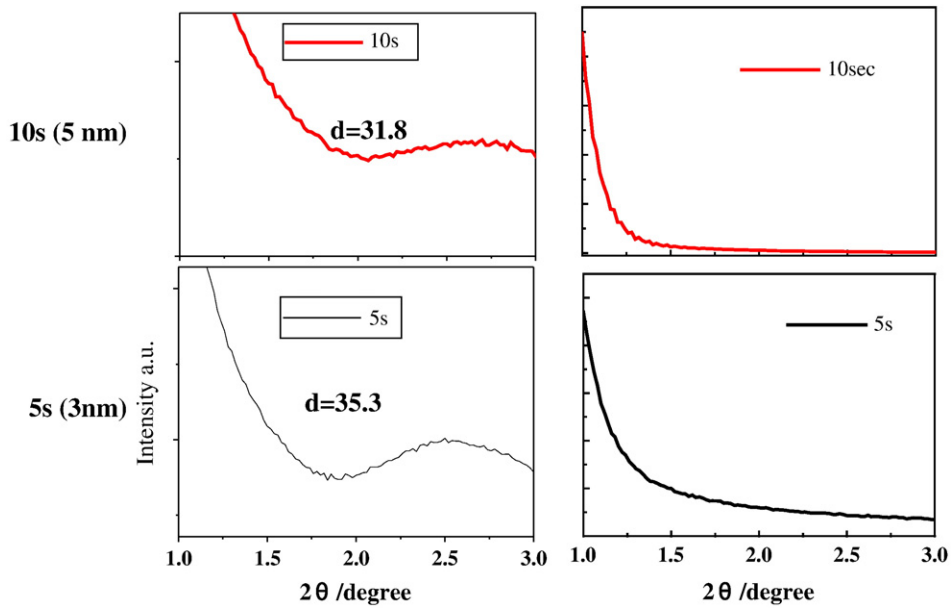

Fig. 6. Small angle XRD pattern of 3- and 5-nm-thick ESD PEDOT:PSS films on c-Si and ITO coated glass.

4. Discussion

As shown in Figs. 3–5, the n_o exhibited metallic behavior in the ordinary, whereas the n_e showed the features more characteristics of a dielectric material as is similar to that of spin-coated films [7]. The uncertainty for the n_e with angle of incidence originates from the fact that the index is probed by a field component of the *p*-polarized light. The anisotropy in the PEDOT layers probably arises from a geometric anisotropy of the polymer chains, whereby a preferential orientation of the chains give rise to uniaxial anisotropy with the optical properties to the sample normal. The measured optical properties might indicate the main part of the polymer chains are lying flat and parallel to the surface plane randomly oriented azimuthally, giving rise to the ordinary index of reflection. The schematic of the film growth on c-SI and ITO coated glass is schematically drawn in Fig. 7. The ESD PEDOT:PSS films on c-Si proceeds with a preferential molecular orientation, whereas the homogenous growth occurs with random orientation on ITO coated glass substrate. These features originate from the sticking process of deposition precursors on substrate.

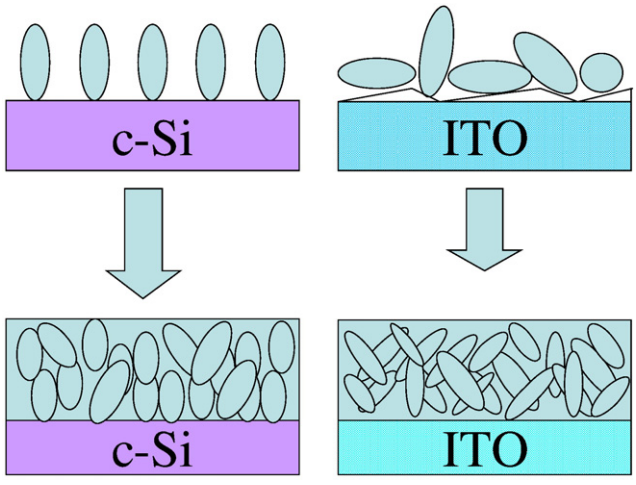

Fig. 7. Schematic of the molecular orientation in the growth on c-Si and ITO coated glass.

5. Conclusions

The uniaxial anisotropic optical property of PEDOT:PSS films by a electrospray deposition (ESD) method was studied using DMF as a solvent solution on c-Si and ITO coated glass through the real-time spectroscopic ellipsometric characterization. The uniaxial anisotropic optical property is prominent on c-Si wafer and depends on the film thickness. These features come from the promotion of the cross-linking reaction and preferential molecular orientation during the film growth. Real-time characterization of optical constants by spectroscopic ellipsometry is a possible method to understand the uniaxial anisotropic optical property and growth kinetics of conjugated polymer thin films by the ESD method.

Acknowledgements

This research was partially supported by Japan Science and Technology (JST) agency (A-step) grant for Scientific Research from the Ministry of Education, Culture, Sports, Science and Technology of Japan.

References

[1] L.B. Groenendaal, F. Jonas, D. Freitag, H. Pielartzik, J.R. Reynolds, Adv. Mater. 12 (2000) 481.
[2] S.K.M. Jonsson, J. Birgerson, X. Crispin, G. Greczynski, W. Osikowicz, A.W. Denier van der Gon, W.R. Salaneck, M. Fahlman, Synth. Met. 139 (2003) 1.
[3] A.M. Nardes, R.A.J. Janssen, M. Kemerink. Adv. Funct. Mater. 18 (2008) 865.
[4] B.L. Groenendaal, F. Jonas, D. Freitag, H. Pielartzik, J.R. Reynolds, Adv. Mater. 12 (2000) 482.
[5] B. Yin, Q. Liu, L. Yang, X. Wu, Z. Liu, Y. Hua, S. Yin, Y. Chen, J. Nanosci. Nanotechnol. 10 (2010) 1934.
[6] S.-I. Na, G. Wang, S.-S. Kim, T.-W. Kim, S.-H. Oh, B.-K. Yu, T. Lee, D.-Y. Kim, J. Mater. Chem. 9 (2009) 9045.
[7] M. Schubert, B. Rheinlander, B. Johs, C.M. Herzinger, J.A. Woollam, J. Opt. Soc. Am. A13 (1996) 875.
[8] L.A.A. Pettersson, F. Carlsson, O. Inganäs, H. Arwin, Thin Solid Films 313–314 (1998) 356.
[9] C. Gravalidis, A. Laskarakis, S. Logothetidis, Eur. Phys. J. Appl. Phys. 46 (2009) 12505.
[10] T. Fukuda, T. Suzuki, R. Kobayashi, Z. Honda, N. Kamata, Thin Solid Films 518 (2009) 575.
[11] G.E. Jellison Jr., F.A. Modine, Appl. Phys. Lett. 69 (1996) 371.
[12] S. D'Elia, N. Scaramuzza, F. Ciuchi, C. Versace, G. Strangi, R. Bartolino, Appl. Surf. Sci. 255 (2009) 7203.
[13] G.E. Jellison Jr., Thin Solid Films 234 (1993) 416.
[14] D.G.M. Anderson, R. Barakat, J. Opt. Soc. Am. A 11 (1994) 2305.